Int. J. Econ. Environ. Geol. Vol. 16 (2) 12-25, 2025
Journal home page: www.econ-environ-geol.org

Open Access
ISSN (Online) 2223-957X

Groundwater Quality Assessment Using Hydrochemical and Multivariate Approaches in Coastal Taluka Shaheed Fazil Rahu, District Badin, Sindh, Pakistan

Ghulam Murtaza Arain[1]*, Tarique Mahmood Noonari[2], Nazia Sattar[1], Sumaira Khatoon[3], Nabeel Ali Khan[1], Nadeem Gul[4], Muhammad Afzal Jamali[5]

[1]Pakistan Council of Research in Water Resources, University Road, Karachi, Pakistan
[2]Pakistan Council of Research in Water Resources, Badin, Pakistan
[3] Centre of Excellence in Marine Biology, University of Karachi, Pakistan
[4]Department of Physics, Sir Syed University of Engineering & Technology, Karachi, Pakistan
[5]Centre for Pure and Applied Geology, University of Sindh, Jamshoro, Pakistan

Corresponding author E-mail:* drmurtaza1977@gmail.com

Abstract: Pakistan ranks 14th among the most water-stressed countries globally, with groundwater (GW) serving as the primary water source for both rural and urban populations. However, GW contamination is a growing concern, driven by excessive agrochemical use, improper wastewater disposal, and toxic elements. Coastal Sindh, particularly District Badin, faces severe water scarcity and deteriorating GW quality, exacerbated by seawater intrusion and the absence of proper water storage and supply infrastructure. This study assesses GW quality in Taluka Shaheed Fazil Rahu (SFR), District Badin, using hydrochemical and multivariate statistical approaches to evaluate contamination sources and freshwater availability. A total of 105 GW samples were acquired from communal bore wells across three union councils and analyzed for physical, chemical, and microbiological parameters. Results showed that 65.71% of samples exceeded turbidity limits, 64.76% had high EC, and 58.1% surpassed TDS thresholds. Microbiological analysis detected total coliforms in 29.52% and *E. coli* in 12.38%, indicating fecal contamination. Contaminants followed the order: Cl^- (56.19%) > HCO_3^- (54.29%) > Na^+ (37.14%) > SO_4^{2-} (31.43%) > K^+ (25.71%) > Mg^{2+} (24.76%) > Ca^{2+} (22.86%) > F^- (14.29%) > As (5.71%) > NO_3^- (1.90%). Multivariate analysis identified salinity (EC, TDS), bicarbonate, chloride, and sodium as primary influences on GW quality. WQI classification showed only 7.62% of samples as excellent, while most were categorized as poor, with UC Tarai (38.46%) having the highest proportion. The findings highlight critical water quality concerns and threats to public health, emphasizing the need for regular monitoring, water treatment, disinfection, and sustainable utilization of resources to ensure safe drinking water.

Keywords: Coastal Sindh, groundwater quality, hydrochemical assessment, multivariate analysis, public health risk, water contamination

Introduction

Pakistan is facing one of the most severe water crises in the world. According to the World Resources Institute, it ranks 14th among countries with extremely high-water stress (WRI, 2019), and more recent assessments place it among the top three water-stressed nations globally (Concern Worldwide, 2023). If effective conservation measures are not adopted, the country's per capita water availability is expected to fall to just 500 cubic meters by 2040 crossing into the threshold of absolute water scarcity (AKU, 2023; Modern Diplomacy, 2024).

Groundwater serves as a critical resource in Pakistan, providing water for domestic use, agriculture, and sustaining ecological systems (Scanlon et al., 2023). Chemically, GW is a complex medium composed of dissolved gases, minerals, organic matter, suspended particles, and colloidal substances (Nikanorov & Brazhnikova, 2009). Its composition is influenced by natural processes such as precipitation, geological formations, rock–water interactions, and climatic factors (Gleeson et al., 2020; Nikanorov & Brazhnikova, 2009). Poor waste disposal practices, such as unlined landfills and open dumping, allow harmful substances to seep into the soil and contaminate the groundwater (EPA, 2015).

In arid and semi-arid regions like Sindh, groundwater remains the primary source of water for both domestic and agricultural purposes due to its accessibility and apparent reliability (Adnan et al., 2019). However, its quality is under growing threat. Both natural processes and human interference are affecting its safety, and it is reported that nearly 68% of the rural population consumes water that falls

below safe quality standards (Memon et al., 2011; PCRWR, 2017; PCRWR, 2021).

Although traditionally considered safer than surface water, GW is now increasingly vulnerable to pollution from industrial discharges, unregulated agricultural runoff, and poor waste management practices (Iqbal & Gupta, 2009).

This is especially true across the Indo-Gangetic plains, where the Sindh province lies. Excessive groundwater pumping, poor regulation, and the growing impact of climate change have led to both declining water tables and increasing contamination. Toxic elements such as arsenic, fluoride, nitrate, and heavy metals—pose serious threats to public health and agricultural sustainability in the region (Haritash et al., 2008; Arain et al., 2007; Arain et al., 2024b; Kumar et al., 2023).

The coastal areas of Pakistan, including the Badin District, face even more serious challenges. Stretching along approximately 350 kilometers of coastline, these areas suffer from severe water scarcity and increasing groundwater salinity. Salinization, driven by seawater intrusion and reduced freshwater input, renders much of the GW unsuitable for human consumption. The lack of water supply infrastructure further exacerbates the problem, placing additional stress on already fragile rural communities (Alamgir et al., 2016; Baloch et al., 2019, Dawn, 2024).

Among these vulnerable areas is Taluka Shaheed Fazil Rahu (SFR) in Badin. Here, the groundwater crisis is intensified by a mix of seawater intrusion, upstream dams and barrages, and a lack of local management. The construction of dams and barrages upstream has significantly reduced freshwater flow to the Indus Delta, exacerbating salinity levels and leading to adverse socioeconomic conditions and widespread GW contamination (Anwar et al., 2014; Mahessar et al., 2015).

In the light of these challenges, there remains a critical need to assess groundwater quality in Taluka Shaheed Fazil Rahu. Despite the region's increasing vulnerability to salinity, seawater intrusion, and contamination, no comprehensive or up-to-date groundwater quality assessment has been conducted in recent years to evaluate its suitability for human consumption. While earlier studies have highlighted groundwater issues in Badin District more broadly (Alamgir et al., 2016; Baloch et al., 2019), but localized investigations focused specifically on Shaheed Fazil Rahu, are still lacking. The absence of such assessments leaves a significant knowledge gap, limiting informed decision-making for water resource management in Taluka SFR.

Therefore, present study aims to fill this gap, using hydrochemical and multivariate statistical approaches to evaluate groundwater quality for human consumption, identify key contamination sources, and provide a comprehensive understanding of the hydrogeochemical processes affecting GW quality in the area.

Materials and Methods

Geology of the Study Area

Badin District is situated in southern Sindh, Pakistan, covering an area of approximately 6,858 km² along the Arabian Sea coastline at coordinates 24.7887° N and 68.9655° E. Geographically, it lies within the coastal and Indus Delta zones, characterized by alluvial plains and deltaic deposits with a mix of sandy and clayey soils (Mahessar et al., 2015). The district experiences a semi-arid to arid climate, with temperatures ranging from around 12°C in winter to over 40°C during the summer months. The mean annual temperature is approximately 26.6°C, and average yearly rainfall about 165 mm, most of which occurs during the monsoon season (PMD, 2019; PMD, 2021). The region is also influenced by maritime winds from the Arabian Sea, which help regulate temperature and humidity levels.

The surface geology of Badin predominantly comprises recent alluvial deposits, with no exposed bedrock in the area (Fig.1). These Holocene deltaic floodplain sediments reflect the presence of ancient meander belts and consist mainly of silt, fine sand, and clay. Stream beds and meander zones contain poorly sorted, fine- to medium-grained sand with minimal clay and silt content. The floodplain is primarily composed of greenish-grey silt and clay with subordinate sand, characteristic of lower terrace deposits.

In the southern Thar Desert, longitudinal sand dunes formed by strong winds are prominent. These dunes, oriented parallel to prevailing wind directions, have short windward slopes and reach thicknesses ranging from 14 to 93 meters. The interdunal areas support sparse vegetation. The sand and silt are moderately to well sorted, primarily composed of quartz, along with minor mica flakes, calcareous soil grains, and fossil fragments.

Badin lies in the lower Indus basin, particularly along southern Sindh which mainly comprises Cretaceous to Tertiary formations with major lithologies of shale, sandstone, limestone, dolomite, clay, and marl (Shah, 2009). Badin area is located in the southwestern periphery of the Indian Plate. The Chiltan Limestone of the Jurassic age is the oldest formation in the Badin block (Jamali et al., 2022)

and is overlain by the Lower Cretaceous marine sand-shale sequence of the Sembar and Goru formations (Wasimuddin et al., 2005). The surface area of Badin district comprises alluvium and sub-Recent deposits without exposure of any outcrop. The generalized stratigraphy (Fig.2) of Lower Indus basin Pakistan including the study area is given by Khan et al. (2016).

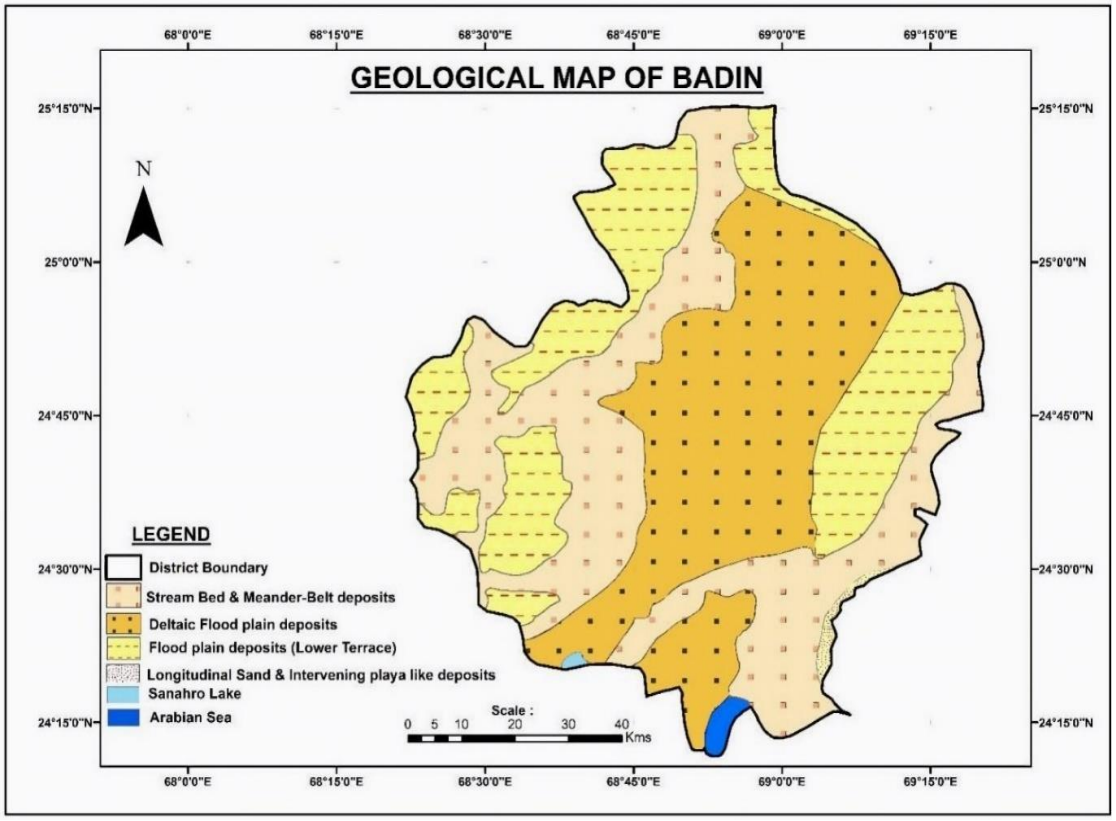

Fig. 1 Geological map of Badin.

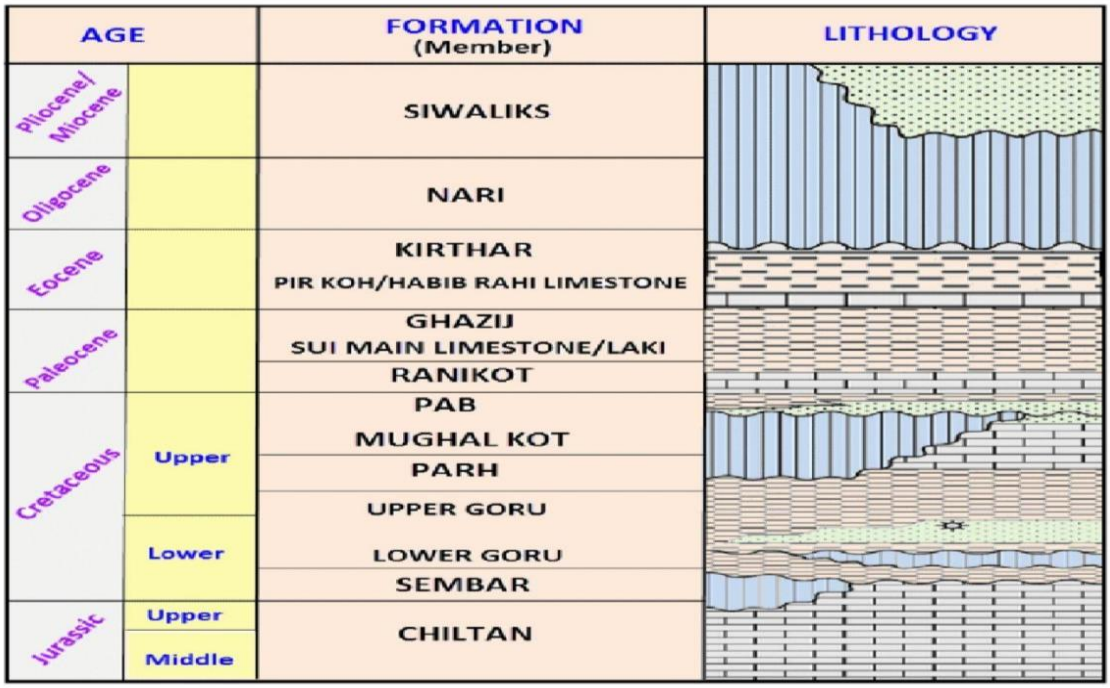

Fig. 2 Stratigraphy of Badin (Khan et al., 2016).

Water Sampling

Groundwater samples (n=105) were collected during March 2024 from shallow bore wells/hand pumps across three union councils (UCs) in Taluka SFR, District Badin (Fig. 3). In UC Khorwah, 37 samples were obtained from 22 villages, with an average bore well depth of 15.62 feet. In UC Tarai, 26 samples were collected from 14 villages, with an average depth of 14.26 feet. Meanwhile, in UC Ahmed Rajo, 42 samples were collected from 25 villages, all from hand pump sources at an average depth of 15.93 feet (Fig. 4). The samples were randomly collected based on the availability of source water following standard procedures for sampling, preservation, and transportation as per the 22nd edition of Standard Methods for the Examination of Water and Wastewater (APHA, 1998).

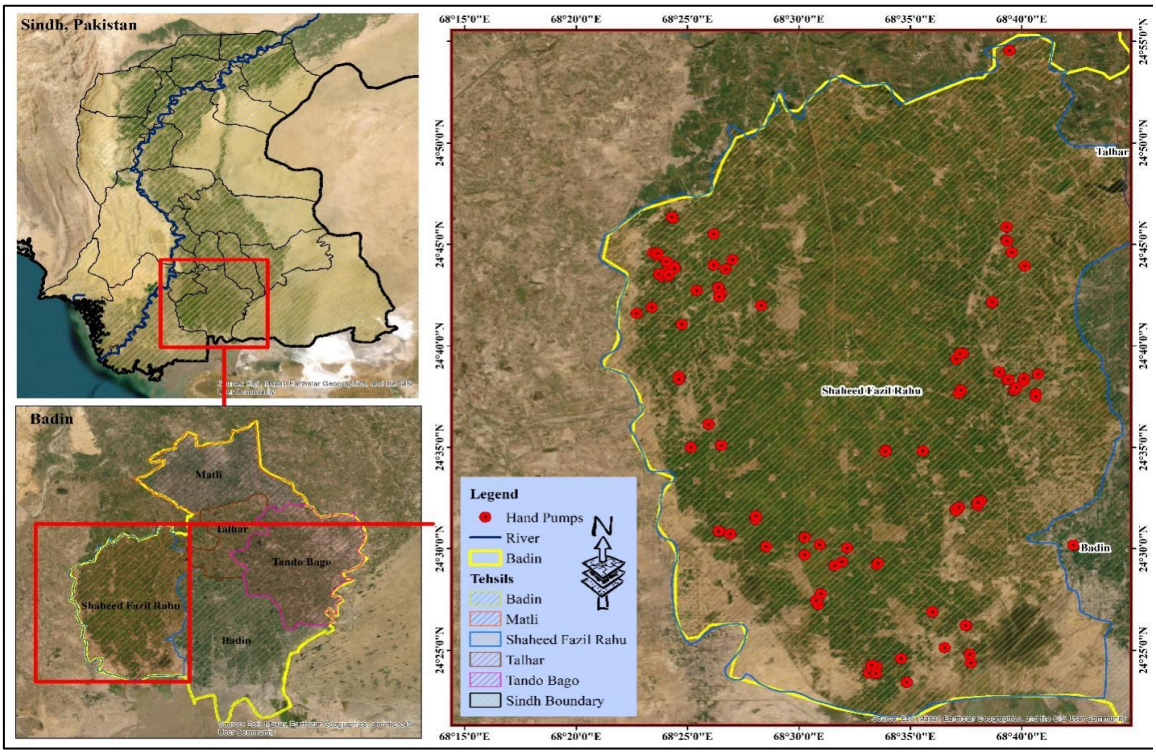

Fig. 3 Location of bore wells/hand pumps within Taluka SFR in District Badin.

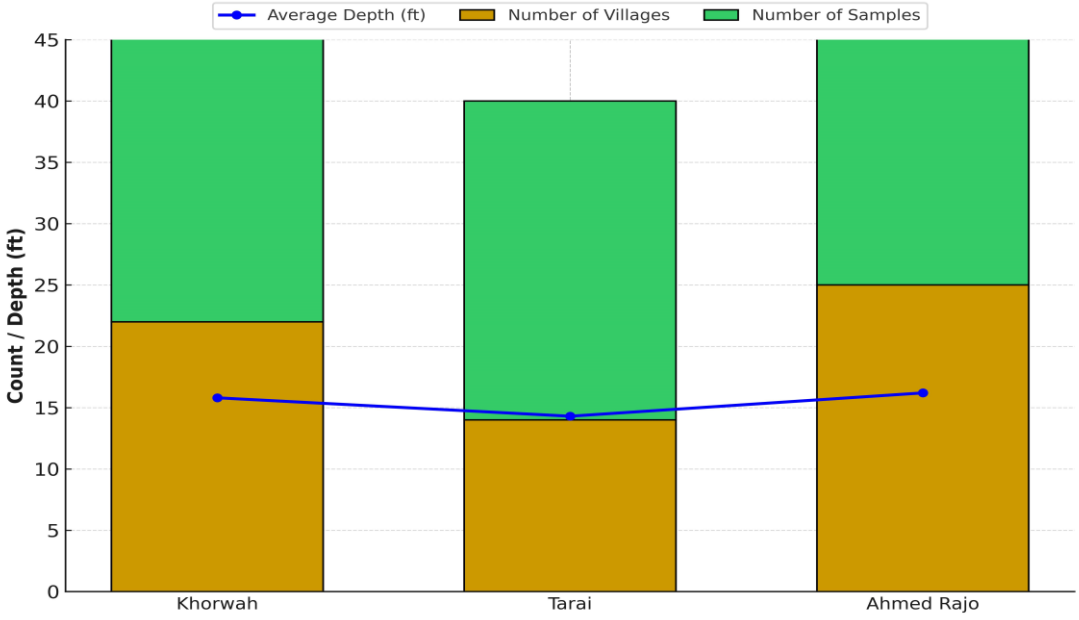

Fig. 4 UC-wise monitoring of villages and water sample collection.

Sample Analysis

Physical and aesthetic parameters, including pH, electrical conductivity (EC), total dissolved solids (TDS), temperature, and GPS coordinates, were measured on-site using the ProDSS Xylem Multi-Parameter Digital Water Quality Meter. Chemical analyses were conducted at the Water Quality Testing Laboratory, Pakistan Council of Research in Water Resources (PCRWR), Badin, Sindh, Pakistan, in accordance with APHA (1998) methods. Sulphates (SO_4^{2-}) and nitrate-nitrogen (NO_3^--N) were analyzed using UV spectrophotometer (Optizen, Korea). Fluoride (F^-) content was determined using the SPADNS method on a Colorimeter (DR-2800, HACH).

Bicarbonates (HCO_3^-) and carbonates (CO_3^{2-}) were measured through titration with 0.02N hydrochloric acid (HCl), while chloride (Cl^-) levels were assessed using the argentometric method with 0.014N silver nitrate ($AgNO_3$) solution. Calcium (Ca^{2+}) and total hardness (TH) were determined volumetrically using 0.01M EDTA titration, while magnesium (Mg^{2+}) concentration was derived using the formula: Mg^{2+} = (TH - 2.5 Ca^{2+}) × 0.243. Potassium (K^+) and sodium (Na^+) were analyzed via a Flame Photometer (Sherwood, UK).

For microbial analysis, the membrane filtration (MF) method was employed to quantify total coliforms (TC) and E. coli. A 100 mL water sample was passed through a 0.45 µm pore-size MF-Millipore membrane for microbial enumeration.

Statistical Analysis

The analysis utilized descriptive and inferential statistics to interpret the data, including comparisons, associations, regression analysis, univariate and multivariate analyses, along with relevant hypothesis testing. Additionally, map construction was carried out using SPSS, ArcMap 10.4, GrapherAqua Plus, and MS Office. To ensure data quality, the charge balance error (CBE) was calculated using Equation (1).

$$\text{CBE} = \frac{\sum \text{cations} - \sum \text{anions}}{\sum \text{cations} + \sum \text{anions}} \times 100 \quad (1)$$

The Water Quality Index (WQI) serves as a practical and straightforward tool for assessing groundwater suitability for drinking purpose (Akter et al., 2016). The WQI calculation follows a systematic approach, assigning weight (w_i), relative weight (W_i), quality rating (Q_i), and computing the sub-index (SI_i) based on Equation (2)**,** as outlined by Arain et al. (2024a, 2024b).

$$WQI = \Sigma SIi \quad (2)$$

Results and Discussion

The analysis of 105 water samples from District Badin reveals significant concerns regarding both physicochemical and microbiological parameters. The pH levels in the analyzed water samples ranged from 7.2 to 8.8, with a mean of 7.92 ± 0.36 SD (Table 1). A total of six samples (5.71%) exceeded the WHO-recommended range of 6.5–8.5 (Fig. 5), indicating slight alkalinity in some water sources.

Table 1. Water quality results in minimum (min), maximum (max), mean with standard deviation (±SD).

Sr. No.	Parameters	Unit	Permissible Limits (WHO)	Min	Max	Mean	±SD
1	pH	-	6.5-6.8	7.2	8.8	7.92	0.36
2	TDS	mg/L	<1000	466.2	9102	1625.49	1447.43
3	Turb.	NTU	<5	0.24	357	27.34	50.20
4	Cl^-	mg/L	250	97	3785	552.00	676.53
5	EC	µS/cm	1500	777	15170	2709.14	2412.38
6	Ca^{2+}	mg/L	150	38	690	130.29	116.36
7	Mg^{2+}	mg/L	100	26	566	94.33	84.35
8	K^+	mg/L	12	5	235	13.17	22.09
9	Na^+	mg/L	200	56	1616	288.32	292.10
10	TH	mg/L	500	190	4050	695.38	616.53
11	SO_4^{2-}	mg/L	250	52	1680	252.15	240.31
12	HCO_3^-	mg/L	300	180	560	312.57	62.63
13	F^-	mg/L	1.5	0.03	3.18	0.96	0.66
14	NO_3^-	mg/L	10	0.5	16.3	2.57	2.56
15	As	µg/L	10	0	50	2.24	8.29
17	TC	CFU	0/100ml	0	150	13.69	26.92
18	*E. coli*	CFU	0/100ml	0	7	0.34	1.09

The pH variations in GW are primarily influenced by natural geochemical processes, including carbonate dissolution, anthropogenic activities, and seawater intrusion in coastal regions (WHO, 2017). Similar studies conducted in coastal Sindh have reported pH values within this range, demonstrating consistency in water chemistry across the region. Memon et al. (2011) recorded pH values between 6.8 and 9.2 in GW samples from southern Sindh, while Baloch et al. (2019) found pH variations ranging from 7.1 to 8.7 in coastal areas of Badin, indicating minor fluctuations due to lithological and environmental factors. A study by Mahessar et al. (2015) in Taluka Badin and SFR also observed comparable results, with pH levels predominantly falling within permissible limits.

Turbidity levels ranged from 0.24 to 357 NTU, with a mean of 27.34 ± 50.20 NTU (Table 1). Sixty-nine samples (65.71%) exceeded the recommended limit of 5 NTU, suggesting potential sediment or microbial contamination (Fig.5). Mahessar et al. (2015) previously reported that 77% of samples from Badin and 45% from SFR Talukas exceeded the safe turbidity limits.

EC values varied from 777 to 15,170 µS/cm, with a mean 2,709.14 ± 2,412.38 µS/cm (Table 1). Sixty-eight samples (64.76%) exceeded the 1,500 µS/cm threshold (Fig. 5), suggesting high ionic concentrations. Comparable studies in coastal Sindh have reported EC values exceeding permissible limits, indicating prevalent salinity issues (Baloch et al., 2019). The TDS concentrations ranged between 466.2 and 9,102 mg/L, averaging 1,625.49 ± 1,447.43 mg/L. Sixty-one samples (58.10%) surpassed the permissible limit of 1,000 mg/L, indicating high mineralization. Mahessar et al. (2015) reported that 47% of samples from SFR Taluka exceeded the safe limits. Similar trends have been observed in other coastal districts, reflecting widespread mineralization concerns (Memon et al., 2011). Cl^- concentrations in the analyzed water samples ranged from 97 to 3,785 mg/L, with an average of 552.00 ± mg/L (Table 1).

A total of 59 samples (56.19%) exceeded the WHO limit of 250 mg/L (Fig.5), suggesting contamination from seawater intrusion, evaporite dissolution, or anthropogenic sources. Studies in coastal Sindh confirm this issue, with Cl^- levels reaching 4,100 mg/L in Badin (Baloch et al., 2019) and 3,500 mg/L in other districts (Nasir et al., 2020).

Mahessar et al. (2015) reported that 47% of samples from SFR Taluka exceeded the safe Cl^- limits. Long-term exposure may not directly harm health but can exacerbate hypertension, especially with high Na^+ levels (Memon et al., 2011). SO_4^{2-} concentrations varied from 52 to 1,680 mg/L, with an average of 252.15 ± 240.31 mg/L (Table 1). Thirty-three samples (31.43%) exceeded the limit of 250 mg/L (Fig. 5), suggesting sources such as gypsum dissolution or industrial discharge. Similar SO_4^2 levels have been observed in coastal districts, indicating common contamination sources (Nasir et al., 2020).

Mahessar et al. (2015) previously reported that 20% of samples from Badin and 37% from SFR Talukas exceeded the safe SO_4^{2-}limits. HCO_3^-concentrations ranged from 180 to 560 mg/L, with a mean of 312.57 ± 62.63 mg/L (Table 1). Fifty-seven samples (54.29%) exceeded the threshold of 300 mg/L (Fig.5), indicating active carbonate dissolution and buffering effects on groundwater alkalinity. Elevated HCO_3^-levels have been reported in coastal regions, reflecting similar geochemical processes (Nasir et al. 2020) which ranged between 38 and 690 mg/L, with an average of 130.29 ± 116.36 mg/L (Table 1). Twenty-four samples (22.86%) exceeded the permissible limit of 150 mg/L (Fig.5), indicating potential GW hardness issues. Comparable findings have been reported in coastal areas, reflecting common hardness concerns (Nasir et al., 2020). The Mg^{2+} levels varied from 26 to 566 mg/L, with a mean of 94.33 ± 84.35 mg/L (Table 1). Twenty-six samples (24.76%) exceeded the recommended limit of 100 mg/L, contributing to increased water hardness. Similar trends have been observed in other coastal districts, indicating prevalent hardness issues (Memon et al., 2011).

Na^+ levels varied from 56 to 1,616 mg/L, averaging 288.32 ± 292.10 mg/L (Table 1). Thirty-nine samples (37.14%) exceeded the WHO limit of 200 mg/L (Fig. 5), indicating potential seawater intrusion or anthropogenic influences. Comparable Na^+ concentrations have been reported in coastal areas, reflecting common contamination concerns (Baloch et al., 2019). Shahab et al. (2016) documented an average Na^+ concentration of 268.20 mg/L and K^+ of 55.64 mg/L in GW from the Lower Indus Plain, Sindh. K^+ concentrations ranged between 5 and 235 mg/L, with an average of 13.17 ± 22.09 mg/L (Table 1). Twenty-seven samples (25.71%) exceeded the permissible limit of 12 mg/L, possibly due to agricultural runoff or mineral dissolution. Elevated K^+ levels have been noted in coastal regions, suggesting similar contamination sources (Nasir et al., 2020). TH values in the analyzed water samples ranged from 190 to 4,050 mg/L, with a mean of 695.38 ± 616.53 mg/L (Table 1). A total of 49 samples (46.67%) exceeded the WHO-recommended permissible limit of 500 mg/L (Fig.5), indicating significant contributions from Ca^{2+} and Mg^{2+} minerals. Elevated hardness in GW results from the dissolution of CO_3^{2-} and SO_4^{2-} minerals, influenced by lithology and rock-water interactions (Memon et al., 2011). Though not

directly harmful, high hardness causes scaling in pipelines and reduces soap efficiency (WHO, 2017). Similar trends in Thatta and Badin show TH levels reaching 3,800 mg/L due to calcium and magnesium (Nasir et al., 2020). Arain et al. (2024a) documented TH levels between 180–2,650 mg/L in District TMK, with an average of 616.8 ± 337.1 mg/L.

F^- levels in the samples ranged from 0.03 to 3.18 mg/L, with an average concentration of 0.96 ± 0.66 mg/L (Table 1). A total of 15 samples (14.29%) exceeded the WHO-recommended limit of 1.5 mg/L (Fig. 5), indicating potential health risks, including dental and skeletal fluorosis. Elevated F^- concentrations in GW are commonly associated with geogenic sources, including weathering of fluoride-rich minerals, as well as anthropogenic activities (Farooqi et al., 2007). Comparable F^- levels have been documented in other coastal regions of Sindh. A study by Memon et al. (2011) in southern Sindh reported F^- concentrations ranging from 0.1 to 4.2 mg/L, with 18% of samples surpassing the permissible limit. Similarly, Nasir et al. (2020) found that F^- levels in some coastal areas exceeded 2.5 mg/L, further highlighting concerns over F^- induced health risks. Long-term exposure to elevated F^- concentrations can lead to severe skeletal deformities, dental mottling, and bone fractures, particularly in vulnerable populations (WHO, 2017).

Nitrate content measured between 0.5 to 16.3 mg/L, with a mean value of 2.57 ± 2.56 mg/L (Table1). Two samples (1.90%) exceeded the WHO permissible limit of 10 mg/L (Fig.5). High NO_3^- concentrations in GW have been widely reported in agricultural areas due to excessive use of fertilizers (Mahessar et al., 2015). A previous study in Sindh reported NO_3^- levels reaching up to 20 mg/L in some coastal districts (Memon et al., 2011). Similarly, Arain et al. (2024a) documented average NO_3^-levels 2.08 ± 1.77 mg/L in GW of neighboring District Tando Muhammad Khan.

Arsenic levels varied between 0 and 50 µg/L, with an average concentration of 2.24 ± 8.29 µg/L (Table 1). Six samples (5.71%) exceeded the WHO recommended guideline of 10 µg/L (Fig. 5), highlighting potential geogenic contamination and associated health risks. Elevated As levels have been reported in GW sources of Sindh, with previous studies indicating concentrations up to 200 µg/L in certain regions (Arain et al., 2007; Farooqi et al., 2007). Long-term consumption of arsenic-contaminated drinking water presents serious health risks, including hyperpigmentation, keratosis, hypertension, heart diseases, and cancers of the skin, bladder, and lungs (Arain et al., 2009; Husain et al., 2012; WHO, 2017).

The contamination levels of anions in this study followed the order Cl^- (56.19%) > HCO_3^- (54.29%) > SO_4^{2-} (31.43%) > F^- (14.29%) > NO_3^- (1.90%), while cation contamination levels were recorded as Na^+ (37.14%) > K^+ (25.71%) > Mg^{2+} (24.76%) > Ca^{2+} (22.86%), respectively. This ionic distribution aligns with previous studies in coastal regions, which have linked elevated Cl^- and Na^+ levels to seawater intrusion and rock-water interactions (Baloch et al., 2019).

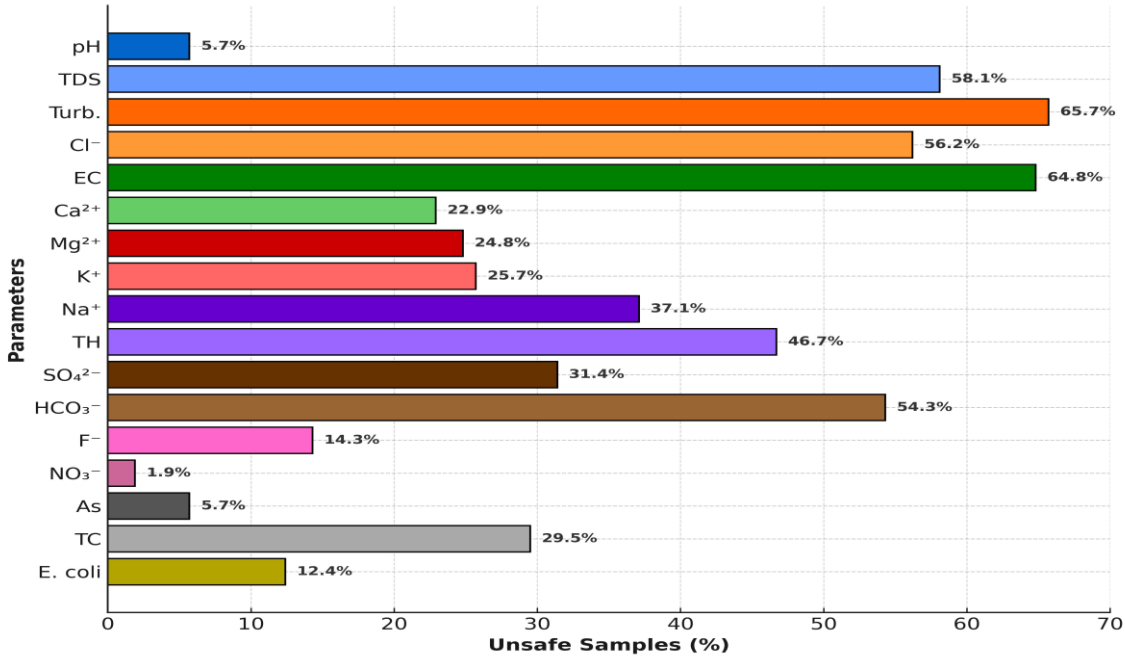

Fig. 5 Proportion (%age) of unsafe samples for different parameters.

TC counts in the water samples ranged from 0 to 150 CFU/100mL, with a mean concentration of 13.69 ± 26.92 CFU/100mL (Table 1). A total of 31 samples (29.52%) tested positive for coliform bacteria (Fig. 5), indicating microbial contamination and potential health risks. The occurrence of TC and *E. coli* in drinking water presents significant health hazards, especially for infants, the elderly, and individuals with weakened immune systems (Nabeela et al., 2014; WHO, 2017). In a similar study conducted in Badin, 34% of water samples were found to contain coliform bacteria, highlighting the widespread issue of microbial contamination in the region (Nasir et al., 2020). *E. coli* contamination was detected in 13 samples (12.38%), with values ranging from 0 to 7 CFU/100mL (mean: 0.34 ± 1.09 CFU/100mL) (Table 1, Fig. 5). The presence of *E. coli* in drinking water is a direct indicator of fecal contamination, posing serious health risks such as gastrointestinal infections (WHO, 2017).

Water Quality Index (WQI)

A total of 105 water samples were analyzed to evaluate the WQI across three UCs; Khor Wah (n = 37), Tarai (n = 26), and Ahmed Rajo (n = 42), located in the SFR sub-district, District Badin. WQI values were categorized as follows: <50 (Excellent), 50–100 (Good), 100–200 (Poor), 200–300 (Very Poor), and >300 (Unsuitable for Drinking) (Tyagi et al., 2013).

Among the analyzed samples, 43 (40.95%) were classified as Good (WQI: 50–100), indicating moderate water quality. Similarly, 33 (34.43%) fell within the Poor category (WQI: 100–200), suggesting declining water quality that requires attention. A smaller fraction, 13 samples (12.38%), was categorized as Very Poor (WQI: 200–300), posing potential health hazards. The affected sample numbers were 7, 13, 33, 40, 44, 45, 48, 52, 57, 58, 66, 78, and 97. Additionally, 8 samples (7.62%) were identified as Unsuitable for Drinking (WQI: >300), reflecting severe contamination requiring immediate remediation. These included samples 16, 34, 42, 51, 76, 82, 83, and 89. Only 8 (7.62%) were categorized as Excellent (WQI: <50), signifying minimal contamination (Fig. 6).

Significant spatial variability in WQ was observed across the UCs. In Khor Wah, the majority of samples (40.54%) were classified as Good, indicating moderate suitability for consumption. However, 29.72% fell within the Poor category, while 8.1% were Very Poor, signaling potential contamination concerns. Additionally, 5.4% of the samples were deemed Unsuitable for Drinking, highlighting the presence of severe pollutants. Encouragingly, 16.21% of the samples were Excellent (Fig.7), representing the quality water among the three UCs.

Ahmed Rajo exhibited the highest proportion of Good quality water (50%), suggesting that half of the sampled sources are safe for consumption.

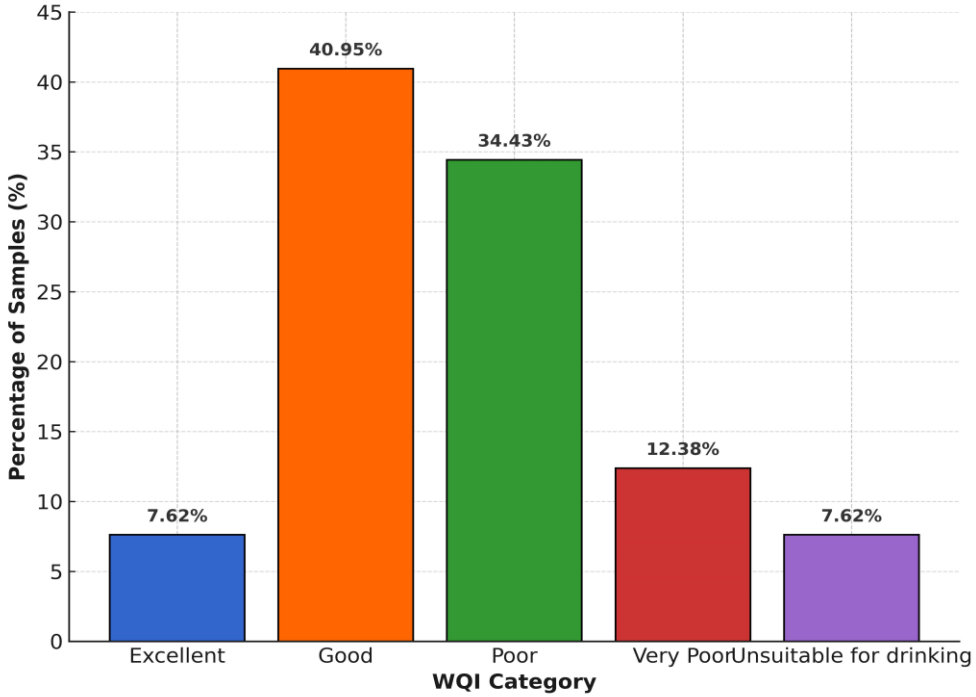

Fig. 6 Proportion of water samples in different WQI categories.

However, 28.57% of the samples were classified as Poor, while 7.14% fell into the Very Poor category, indicating deteriorating WQ. Notably, 9.52% of the samples were Unsuitable for Drinking, marking the highest proportion of unsafe water among the UCs. Only 4.76% of the samples were Excellent, emphasizing limited access to high-quality water sources (Fig. 7).

Tarai demonstrated the poorest WQ among the three UCs. No samples were categorized as Excellent, indicating a complete absence of pristine water sources. The largest proportion (38.46%) fell within the Poor category, while 26.92% were Very Poor, highlighting significant water degradation. Additionally, 7.69% of the samples were Unsuitable for Drinking, emphasizing a critical need for immediate intervention. The Good category accounted for only 26.92%, suggesting that while some water sources remain acceptable, the overall WQ in Tarai is substantially compromised.

Groundwater Facies Analysis

The hydrochemical assessment of GW facilitates the classification of hydrochemical facies by analyzing the distribution of major cations (Ca^{2+}, Mg^{2+}, Na^{+} + K^{+}) and anions (Cl^{-}, SO_4^{2-}, HCO_3^{-} + CO_3^{2-}), along with their geochemical interactions and governing processes. The Piper diagram reveals that Na^{+} + K^{+} is the dominant cation (38–55%) (left triangle), indicating strong cation exchange, where Ca^{2+} and Mg^{2+} are replaced by Na^{+}, a characteristic of clay-rich aquifers. Ca^{2+}follows (22–34%) reflecting carbonate dissolution from limestone, dolomite or gypsum-bearing formations. Mg^{2+}concentrations (14–28%) suggest limited dolomite dissolution (Fig. 8).

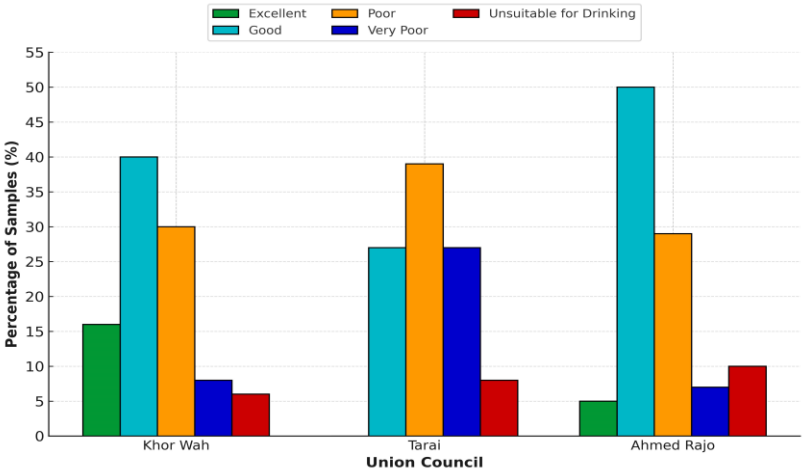

Fig. 7 WQI classification of water samples union council wise in SFR

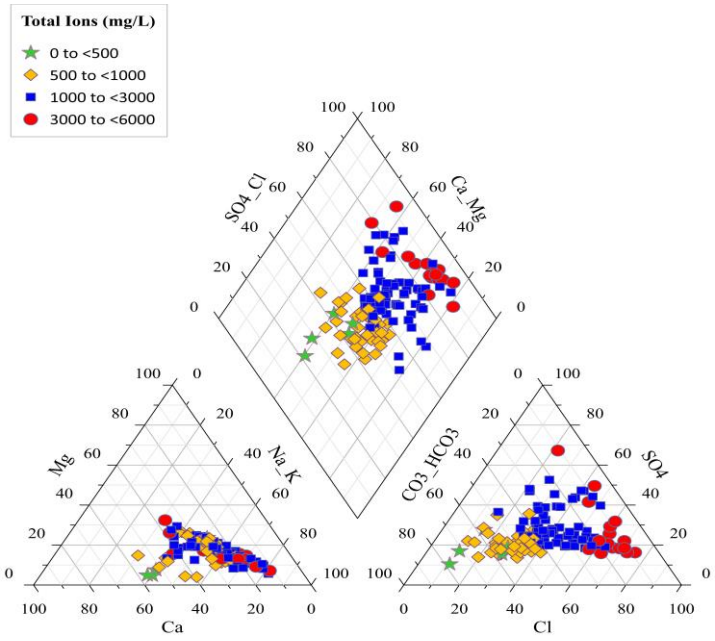

Fig. 8 Piper diagram showing classification of groundwater facies.

Among anions, HCO_3^- + CO_3^{2-} predominate (44–50%), lower right triangle signifying carbonate weathering and CO_2 dissolution as key controls on GW chemistry. Cl^- (30–38%) suggests possible seawater intrusion, evaporation, or anthropogenic contamination. SO_4^{2-} (15–25%) indicates gypsum or anhydrite dissolution. The Na^+ - HCO_3^- facies dominates, signifying geochemical evolution driven by silicate weathering, ion exchange, and carbonate dissolution, typical of inland freshwater systems. However, a subset of samples trends toward the Na^+ - Cl^- facies, indicating potential salinity risks from seawater intrusion, evaporative concentration, or anthropogenic inputs.

Hydrochemical interactions confirm that $Na^+ + K^+$ dominance over Ca^{2+} and Mg^{2+} supports active cation exchange, leading to increased Na^+ and depletion of Ca^{2+} and Mg^{2+}. High HCO_3^- concentrations highlight CO_3^{2-}weathering as a major contributor to alkalinity. The presence of Cl^-rich waters in some areas suggests salinity intrusion, while moderate SO_4^{2-} levels indicate gypsum dissolution and agricultural impacts.

Determination of Coefficient of Correlation

The Pearson correlation analysis among physical and chemical parameters (n=15) were calculated using IBM SPSS Statistics25 software which provides valuable insights into the interactions between anions and cations, highlighting key geochemical processes and anthropogenic influences shaping GW composition. A strong positive correlation (r > 0.90) is identified between Ca^{2+} and Cl^- (r = 0.902), Ca^{2+} and EC (r = 0.933), Ca^{2+} and TH (r = 0.964), Cl^- and EC (r = 0.985), Cl^- and TDS (r = 0.985), and Mg^{2+} and TH (r = 0.990) (Table 2). These relationships indicate that Ca^{2+}, Mg^{2+}, Cl^-, and TH significantly contribute to EC and TDS, underscoring the role of $CO_3^{2-}$and Cl^- mineral dissolution. The high correlation between TH and both Ca^{2+} and Mg^{2+} suggests that GW hardness is primarily controlled by these cations.

Moderate correlations (r = 0.60–0.89) are observed between Na^+ and Cl^- (r = 0.953), Na^+ and EC (r = 0.952), Na^+ and SO_4^{2-} (r = 0.878), SO_4^{2-} and EC (r = 0.954), and NO_3^- and EC (r = 0.928) (Table 2). These associations point to Na^+- Cl^- dissolution and potential anthropogenic influences, such as agricultural runoff or wastewater infiltration. The notable correlation between NO_3^- and EC suggests nitrate contamination, likely from excessive fertilizer application.

Weak correlations (r < 0.50) are observed between F^- and most parameters (maximum r = 0.420 with TH and Mg^{2+}), indicating that F^- levels are not significantly influenced by major ions. Similarly, weak correlations with all parameters (maximum r = 0.234 with pH), implying; that mobility is governed by redox conditions rather than direct ion interactions. Negative correlations between pH and major ions, particularly pH vs Na^+ (r = -0.167), pH vs Cl^- (r = -0.128), and pH vs EC (r = -0.142) (Table 2), suggest that increasing ionic concentrations coincide with lower pH values, facilitating mineral dissolution. Overall, GW chemistry in SFR, Badin, is primarily influenced by $CO_3^{2-}$and SO_4^{2-} mineral dissolution, ion exchange, and potential anthropogenic inputs. Strong correlations among Ca^{2+}, Mg^{2+}, Cl^-, SO_4^{2-}, and EC indicate geogenic dominance, while the NO_3^--EC correlation highlights human-induced contamination.

Table 2. Correlation coefficient of WQ parameters analyzed in SFR, Badin.

	HCO_3^-	Ca^{2+}	Turb	Cl^-	EC	TH	Mg^{2+}	pH	K^+	Na^+	SO_4^{2-}	TDS	NO_3^-	F^-	As
HCO_3^-	1.000														
Ca^{2+}	0.639	1.000													
Turb	-0.015	-0.032	1.000												
Cl^-	0.589	**0.902**	-0.046	1.000											
EC	0.631	**0.933**	-0.038	**0.985**	1.000										
TH	0.609	**0.964**	-0.039	0.914	0.943	1.000									
Mg^{2+}	0.596	0.952	-0.025	0.915	0.944	**0.990**	1.000								
pH	-0.115	-0.088	0.096	-0.128	-0.142	-0.129	-0.114	1.000							
K^+	0.136	0.067	-0.063	0.075	0.080	0.076	0.079	-0.047	1.000						
Na^+	0.578	0.791	-0.043	**0.953**	**0.952**	0.806	0.807	-0.167	0.078	1.000					
SO_4^{2-}	0.557	0.902	-0.039	0.919	**0.954**	0.942	0.943	-0.140	0.089	**0.878**	1.000				
TDS	0.631	0.933	-0.038	**0.985**	1.000	0.943	0.944	-0.142	0.080	0.952	0.954	1.000			
NO_3^-	0.628	0.927	-0.041	0.883	**0.928**	0.914	0.919	-0.097	0.085	0.830	0.898	0.928	1.000		
F^-	0.414	0.403	0.065	0.346	0.363	0.420	0.420	0.149	0.020	0.272	0.349	0.363	0.354	1.000	
As	0.105	0.066	0.028	0.048	0.046	0.103	0.112	0.234	-0.021	-0.004	0.037	0.046	0.020	0.389	1.000

Principal Component Analysis (PCA)

The PCA of GW quality data identifies key hydrochemical processes influencing water composition. PC1 (60.08% variance) is

predominantly driven by EC, TDS, HCO_3^-, Cl^-, and Na^+, indicating that GW quality is primarily controlled by salinity and dissolved mineral content. This suggests evaporation, seawater intrusion, and excessive GW extraction as major contributors to elevated salinity levels. The strong loading of Cl^- and Na^+ further supports the influence of marine aerosols and ion exchange processes on GW chemistry (Table 3).

PC2 (10.26% variance) is strongly associated with pH and turbidity, emphasizing the role of alkalinity, organic matter, and suspended particles. These variations may be linked to carbonate equilibrium, sediment transport, and anthropogenic pollution. PC3 (7.01% variance) exhibits high loadings for SO_4^{2-} and turbidity, indicating potential industrial and agricultural runoff and wastewater discharge.

PC4 (6.28% variance) is influenced by Ca^{2+} and Mg^{2+}, contributing to GW hardness, likely due to CO_3 dissolution from limestone or gypsum deposits. 5.47% variance negatively correlates with pH and F^-, suggesting geogenic F^- contamination, potentially from fluorite-bearing minerals. K^+ presence, though, less dominant, may be linked to silicate weathering and agricultural inputs. The PCA analysis highlights salinity intrusion, mineral dissolution, industrial and agricultural contamination, and geogenic influences as key factors affecting GW quality in Taluka SFR. The Scree Plot shows a declining variance trend, with PC1 (60.09%) as the most significant factor (Fig. 9).

Table 3. PCA loading factor analysis for variable parameters.

Parameters	PC1	PC2	PC3	PC4	PC5	PC6	PC7	PC8	PC9	PC10
EC	0.330	-0.045	-0.040	-0.010	-0.051	0.064	-0.014	-0.159	0.006	-0.076
pH	-0.050	0.504	-0.067	-0.031	-0.810	-0.225	-0.153	-0.031	0.067	0.028
Turb	-0.015	0.205	-0.590	0.762	0.123	0.113	-0.036	0.008	-0.004	-0.004
TDS	0.330	-0.045	-0.040	-0.010	-0.051	0.064	-0.014	-0.159	0.006	-0.076
HCO_3	0.227	0.080	0.176	0.116	0.309	-0.532	-0.698	0.041	0.140	0.091
Cl^-	0.322	-0.046	-0.045	-0.023	-0.076	0.098	-0.002	-0.285	0.152	-0.386
SO_4^{2-}	0.319	-0.049	-0.041	-0.010	-0.074	0.113	0.119	0.040	0.245	0.746
Ca^{2+}	0.319	0.019	-0.030	-0.013	-0.048	-0.041	0.028	0.369	-0.028	-0.487
Mg^{2+}	0.322	0.031	-0.024	-0.013	-0.025	0.074	0.121	0.322	0.220	0.059
TH	0.323	0.021	-0.017	-0.023	-0.010	0.053	0.113	0.338	0.274	-0.042
Na^+	0.303	-0.110	-0.050	-0.004	-0.061	0.100	-0.108	-0.642	-0.090	0.044
K^+	0.033	-0.095	0.738	0.615	-0.200	0.130	0.095	-0.004	-0.007	-0.025
NO_3	0.315	-0.024	-0.028	0.003	-0.085	-0.053	-0.028	0.218	-0.868	0.171
F^-	0.142	0.525	0.138	0.010	0.319	-0.431	0.588	-0.222	-0.050	0.003
As	0.027	0.624	0.202	-0.159	0.246	0.631	-0.279	0.019	-0.067	0.008

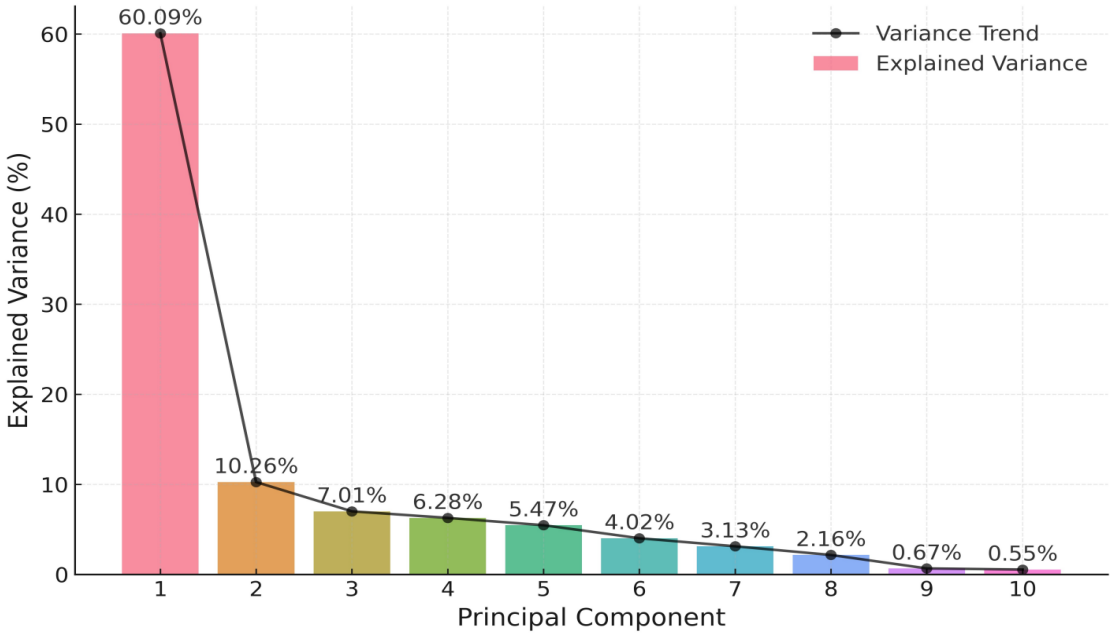

Fig. 9 Scree plot explained variance (%) VS principal components.

Cation and Anion Balance

The ionic balance analysis of GW chemistry in SFR, Badin, reveals a near-equilibrium state, with total cations (27.142 Meq/L) and anions (26.126 Meq/L) closely aligned (Fig.10). The calculated ionic balance error of 3.81% is within the acceptable range for natural waters, confirming a well-maintained charge balance. Na^+ and Cl^- dominate the composition, suggesting halite dissolution or seawater intrusion, while Ca^{2+}, Mg^{2+}, SO_4^{2-}, and HCO_3^- indicate CO_3^{2-} and SO_4^{2-} mineral dissolution. The low error percentage validates the dataset's reliability, ensuring its suitability for hydrochemical interpretations related to water quality and geochemical processes.

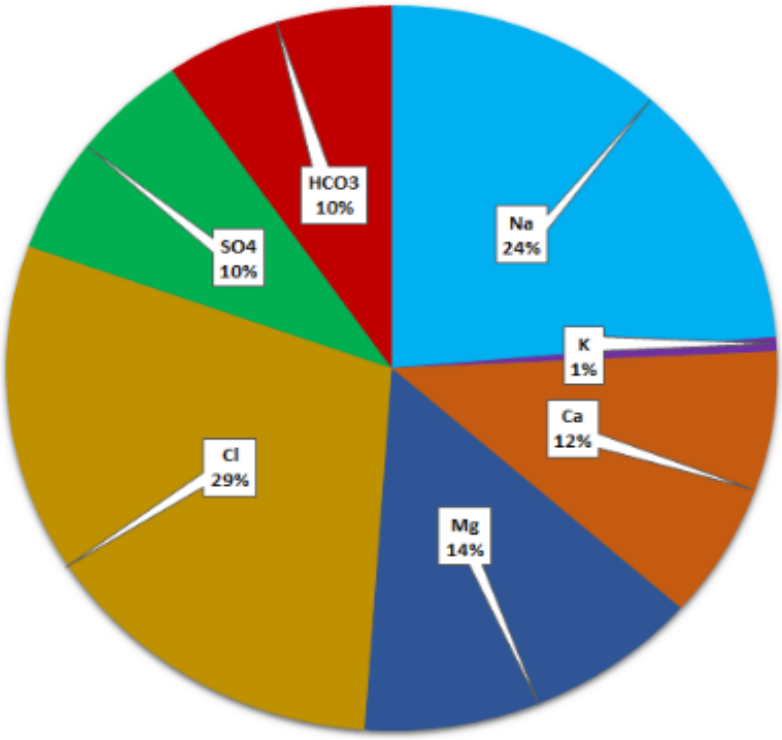

Fig. 10 Ionic balance among cations vs anions.

Conclusion

Groundwater samples (n = 105) were collected from communal bore wells across three union councils of Taluka SFR, District Badin, Sindh, and analyzed for physical, chemical, and microbiological parameters, including pH, TDS, turbidity, Cl^-, EC, Ca^{2+}, Mg^{2+}, K^+, Na^+, TH, SO_4^{2-}, CO_3^{2-}, HCO_3^-, F^-, NO_3^-, As, total coliforms, and *E. coli*. The analytical results indicated that 65.71% of samples were unsafe due to excessive turbidity, followed by 64.76% exceeding permissible EC levels and 58.1% surpassing TDS limits. Microbiological analysis revealed that total coliform bacteria were present in 29.52% of samples, while E. coli, a fecal contamination indicator, was detected in 12.38% of samples.

Multivariate analysis was applied to assess GW hydrochemistry and quality. WQI classification showed that only 8 samples (7.62%) were categorized as Excellent (WQI <50), while the majority of samples were classified as Poor, with the highest proportion in UC Tarai (38.46%), followed by Khor Wah (29.72%) and Ahmed Rajo (28.57. The findings raise serious concerns about GW quality in Shaheed Fazil Rahu, particularly elevated turbidity, salinity, and microbial contamination, which pose significant public health risks.

References

Adnan, S., Iqbal, J. (2019). Spatial analysis of the groundwater quality in the Peshawar District, Pakistan. *Environmental Earth Sciences,* **78**(3), 1-16.

Akter, T., Jhohura, F. T., Akter, F., Chowdhury, T. R., Mistry, S. K., Dey, D., Barua, M. K., Islam,

M. A., Rahman, M. (2016). Water quality and health status of urban slum dwellers in Bangladesh. *Journal of Health, Population and Nutrition*, **35**(4). https://doi.org/10.1186/s41043-016-0041-5

AKU (2023). Pakistan among world's most water-stressed countries. Retrieved from https://www.aku.edu/news/Pages/News_Details.aspx?nid=NEWS-002910

Alamgir, A., Khan, M. A., Schilling, J., Shaukat, S. S., Shahab, S. (2016). Assessment of groundwater quality in the coastal area of Sindh province, Pakistan. *Environment monitoring and assessment*, **188**, 78. https://doi.org/10.1007/s10661-015-5061-x

Anwar, M. M., Chandio, N. H., Bhalli, M. N. (2014). Economic deprivation of Indus River Delta, Sindh, Pakistan: Causes and suggestions. *Science International* (Lahore), **26**(2), 885–890. ISSN 1013-5316.

APHA (1998). Standard methods for the examination of water and wastewater. American Public Health Association, 23rd edition. Washington DC.

Arain, G. M., Aslam, M., Majidano, S. A. (2007). A preliminary study on the arsenic contamination of underground water. *Journal of the Chemical Society of Pakistan*, **29**(5), 463–466.

Arain, G. M., Sattar, N., Khatoon, S., Mustaquim, J. (2024a). Assessment of groundwater quality of Taluka Bulri Shah Karim, District Tando Muhammad Khan, Sindh, Pakistan. *International Journal of Economic and Environmental Geology*, **14**(3), 9–19.

Arain, G. M., Khatoon, S., Sattar, N., Mustaquim, J. (2024b). Assessment of groundwater quality and hydrochemistry using water quality index in District Mirpur Khas, Sindh, Pakistan. *Asian Journal of Chemistry*, **36**(10), 2405–2415.

Arain, M., Kazi, T., Baig, J., Jamali, M., Afridi, H., Shah, A., Jalbani, N., Sarfraz, R. (2009). Determination of arsenic levels in lake water, sediment, and foodstuff from selected area of Sindh, Pakistan: Estimation of daily dietary intake. *Food and Chemical Toxicology*, **47**(2), 242–248.

Baloch, S., Chang, F. K., Hafeez-ur-Rehman Mangio, M. S., Ismail, M. (2019). Deterioration of ground water quality through seawater intrusion in coastal area of District Badin, Sindh Pakistan. *International Journal of Environmental Sciences & Natural Resources*, **20**(5), 148-157.

Concern Worldwide (2023). Countries facing water scarcity and stress. Retrieved from https://www.concern.net/news/countries-with-water-stress-and-scarcity

Dawn (2020). Sindh's agricultural challenges and irrigation dependency. Retrieved from https://www.dawn.com/news/1589272

Dawn (2024).Water crisis in the Indus Delta: Challenges and consequences**.** Retrieved from https://www.dawn.com/news/1895480

Environmental Protection Agency (2015). Groundwater contamination and its impact on drinking water supplies. Retrieved from https://www.epa.gov/sites/default/files/2015-08/documents/mgwc-gwc1.pdf

Farooqi, A., Masuda, H., Firdous, N. (2007). Toxic fluoride and arsenic contaminated groundwater in the Lahore and Kasur districts, Punjab, Pakistan and possible contaminant sources. *Environmental Pollution*, **145**(3), 839-849.

Gleeson, T., Cuthbert, M., Ferguson, G., Perrone, D. (2020). Global groundwater sustainability, resources, and systems in the Anthropocene. *Annual Review of Earth and Planetary Sciences*, **48**, 431-463.

Haritash, A. K., Kaushik, C. P., Kaushik, A., Kansal, A., Yadav, A. K. (2008). Suitability assessment of groundwater for drinking, irrigation and industrial use in some North Indian villages. *Environmental monitoring and assessment*, **145**, 397-406.

Husain, V., Naseem, S., Khan, A., Bhattacharya, P., Arain, G. M. (2012). Natural arsenic in groundwater of Indus delta in the province of Sindh, Pakistan. In: Understanding the Geological and Medical Interference of Arsenic-Ng. Taylor & Francis Group, London.

Iqbal, M. A., Gupta, S. G. (2009). Studies on heavy metal ion pollution of ground water sources as an effect of municipal solid waste dumping. *African Journal of Basic and Applied Sciences*, **1**(5-6), 117-122.

Jamali, M. A., Markhand, A. H., Agheem, M. H., Shafqat, H. Z., Wali, A. Y. (2023). Spatial variation in groundwater quality with respect to surface water seepages in Kadhan area District Badin (Indus Delta), Sindh, Pakistan. *Int. J.*

Energ. Water Res., **7**, 105–117. https://doi.org/10.1007/s42108-022-00211-2

Mahessar, A. A., Memon, N. A., Leghari, M. E. H., Qureshi, A. L., Arain, G. M. (2015). Assessment of source and quality of drinking water in coastal area of Badin, Sindh, Pakistan. *IOSR Journal of Environmental Science, Toxicology and Food Technology*, **9**(1), 1-6.

Khan, M., Nawaz, S., Shah, M., Hasan, M. (2016). Interpreting seismic profiles in terms of structure and stratigraphy, an example from Lower Indus Basin Pakistan. *Universal Journal of Geoscience* (Case Publication), **4**(3), 62 - 71. DOI: 10.13189/ujg.2016.040302.

Memon, M., Soomro, M. S., Akhtar, M. S., Memon, K. S. (2011). Drinking water quality assessment in southern Sindh (Pakistan). *Environmental Monitoring and Assessment*, **177**(1-4), 39–50.

Modern Diplomacy (2024). Projected water security of Pakistan. Retrieved from https://moderndiplomacy.eu/2024/08/07/projected-water-security-of-pakistan

Nabeela, F., Azizullah, A., Bibi, R., Uzma, S., Murad, W., Shakir, S. K., Häder, D. P. (2014). Microbial contamination of drinking water in Pakistan: A review. *Environmental Science and Pollution Research*, **21**, 13929-13942. https://doi.org/10.1007/s11356-014-3348-z

Nasir, M. I., Abbasi, H. N., Zubair, A., Ahmad, W. (2020). Seasonal assessment of water quality by statistical analysis in the coastal area of Sindh, Pakistan. *Pakistan Journal of Scientific & Industrial Research Series A: Physical Sciences*, **63**(2), 130-138.

Nikanorov, A. M., Brazhnikova, L. V. (2009). Water chemical composition of rivers, lakes and wetlands. *Types and properties of water*, **2**, 42-80.

Pakistan Council of Research in Water Resources (2017). Water quality status of major cities of Pakistan, *2015-16*, PCRWR.

Pakistan Council of Research in Water Resources (2021). Drinking water quality in Pakistan: Current status and challenges. PCRWR, Ministry of Science and Technology, Government of Pakistan. Retrieved from https://pcrwr.gov.pk/wp-content/uploads/2023/08/Drinking-Water-Quality-in-Pakistan-Current-Status-and-Challenges.pdf

Pakistan Meteorological Department (2019). State of Pakistan's climate in 2019. Climate data processing center, Karachi. Retrieved from www.pmd.gov.pk

Pakistan Meteorological Department (2021). Climate data for Badin District. Retrieved from www.pmd.gov.pk

Scanlon, B. R., Fakhreddine, S., Rateb, A., de Graaf, I., Famiglietti, J., Gleeson, T., Zheng, C. (2023). Global water resources and the role of groundwater in a resilient water future. *Nature Reviews Earth & Environment*, **4**(2), 87-101.

Shah, S. M. I. (2009). Stratigraphy of Pakistan. *Memoirs of the Geological Survey of Pakistan*, **22**, 240 pages.

Shahab, A., Shihua, Q., Rashid, A., Ul Hasan, F., Sohail, M. T. (2016). Evaluation of water quality for drinking and agricultural suitability in the Lower Indus Plain in Sindh Province, Pakistan. *Polish Journal of Environmental Studies*, **25**(6), 2563–2574. https://doi.org/10.15244/pjoes/63777

Tyagi, S., Sharma, B., Singh, P., Dobhal, R. (2013). Water quality assessment in terms of water quality index. *American Journal of Water Resources*, **1**(3), 34-38.

Wasimuddin, M., Jadoon, I. A. K., Weihua, W., Akhtar, S., Ebdon, C. C. (2005). Integration of image logs in the structural analysis of the Zaur Field, Lower Indus Basin, Pakistan. Presented at the PAPG/SPE Annual Technical Conference, Islamabad, Pakistan.

World Health Organization (2011). Guidelines for drinking water quality, Geneva.

World Health Organization (2017). Guidelines for drinking-water quality (4th Ed.). Geneva, Switzerland, WHO Press.

World Resources Institute (WRI). (2019). *World's water-stressed countries ranking*. Retrieved from https://www.wri.org/insights/highest-water-stressed-countries